Source-geophone azimuth from 3-C seismic polarization

Saul E. Guevara and Robert R. Stewart

ABSTRACT

The source-geophone azimuths from an offset source shot into a 3-C seismic line (over the Blackfoot field, Alberta) are determined using polarization analysis. We find that the refracted *S*-wave arrivals, *P*-*S* reflections, and ground roll all give good estimates of the actual shot-receiver geometry. First-breaking *P*-wave energy does not provide a consistent direction of arrival.

INTRODUCTION

We are interested in the polarization of various events in the recorded multicomponent data to help determine the event type (*P*, *S*, Rayleigh) as well as the direction of the events' arrival. The polarization properties can also be used to filter unwanted modes and arrival angles or be used in checking the plant orientation of the geophone. Bland and Stewart (1996) proposed to use polarization for geophone orientation on land 3-C seismic data. Estimating the azimuth of the arrival direction from the recorded data alone could provide a means to check the actual shooting geometry and geophone plant orientation. In this study, we analyze polarization and geophone orientation from data of the Blackfoot III 3C-2D seismic survey (Hoffe et al., 1998). Three analysis methods are used: hodograms, histograms (DiSiena et al, 1984) and covariance matrix (Flinn, 1965).

BLACKFOOT SEISMIC DATA ANALYSIS

The Blackfoot survey data

The CREWES Project conducted a high-resolution 3-C seismic line over the Blackfoot oilfield, Alberta, in 1997. A shot gather from the high-resolution seismic line, with 1 km length and 2 m distance between geophones, was used to carry out this analysis. Figure 1 illustrates the receiver locations. In the field survey, several shots were offset from the line. We use a shot 48 m offset from the geophone line for this analysis. One hundred and seventy one receivers symmetrical in relation to the source were used, forming a 340 m *split-spread* geometry.

Figure 2 illustrates the data set and the four events selected with the corresponding analysis windows. Event 1 corresponds to first-arriving *P*-wave energy, with an apparent velocity of 2300 m/s. Event 2 appears to be parallel to event 1 and is stronger on the horizontal components. Event 3 was selected from the radial component and has an apparent velocity close to 800 m/s. The apparent velocity of event 4 (ground roll) is approximately 360 m/s.

Analysis method

Two types of analysis are performed on the data. The first one is a hodogram analysis of five traces, which includes results from the histogram and covariance matrix methods. The second one is a covariance matrix analysis of all the traces.

The analyses of the first type are presented in matrix-like form (Figs. 3 to 6), where each row corresponds to a receiver, column *a* corresponds to the lateral view hodogram, column *b* to the top view hodogram, and column *c* to the histogram of the horizontal components. Table 1 shows the source-to-receiver azimuth of the five receivers according to the acquisition geometry. In the second analysis the azimuths from the field survey are compared with the resulting polarization direction from the covariance matrix method (Figs. 7 to 10). For each polarization angle calculated, the azimuthally opposite is assumed.

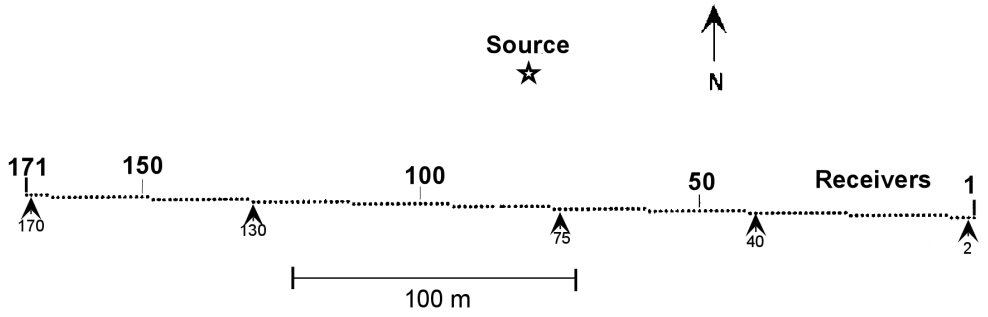

Figure 1. Field layout of the test data from Blackfoot III 3C-2D. The source is 48 m offset from the line of receivers. Numbers on the line identify receivers and the receivers selected for testing are indicated with arrows.

Table 1. Azimuth from the acquisition geometry in Blackfoot III

Receiver Number	*Offset (m)*	*Azimuth*
2	166.7	163.27º
40	96.6	150.21º
75	50.4	107.75º
130	108.3	26.31º
170	183.1	15.2º

RESULTS

Hodogram analysis

The hodogram analyses of the four events are illustrated in Figures 3 to 6. Columns *a* and *b* are the hodograms and column *c* the histogram. The arrowheads in column *c* indicate the theoretical azimuth according to the field geometry. Factor *fl*, the linearity from the covariance matrix method, is also in column *c*. In the hodograms the horizontal components are labeled with *R* (radial or *in-line*), *T* (transverse or *cross-line*), or *V* (vertical). From the field layout, the radial (*R*) or in-line component positive direction is oriented toward the East (Fig. 1). The azimuth is calculated counter-clockwise from this direction.

The side view hodogram of event 1 (Figure 3a) shows higher linearity and more energy than the top view hodogram (Figure 3b). These characteristics, together with the apparent velocity (Fig. 2a), identify this event as a *P* refracted wave. In the top view hodogram (Fig 3b) the linearity and the correlation with the source-receiver direction are low.

The second event (Figure 4) shows high energy content in the horizontal components, high linearity and good correlation of the polarization angle with the azimuth source-receiver. The arrowheads in column *c* show near correlation with the direction obtained from the histogram. The second event apparent velocity corresponds to the velocity of the first event; however its polarization is highly horizontal, which may correspond to a converted *S*-wave created by the *P*-wave refraction.

Table 2. Azimuth S-R versus polarization angle.

Receiver Number	*Azimuth*	*Polarization angle*			
	S-R	Event 1	Event 2	Event 3	Event 4
2	163º	152°	159º	168º	168º
40	150º	92°	146º	157º	145º
75	108º	104°	96º	94º	124º
130	26º	2°	29º	34º	25º
170	15º	9°	41º	8º	6º

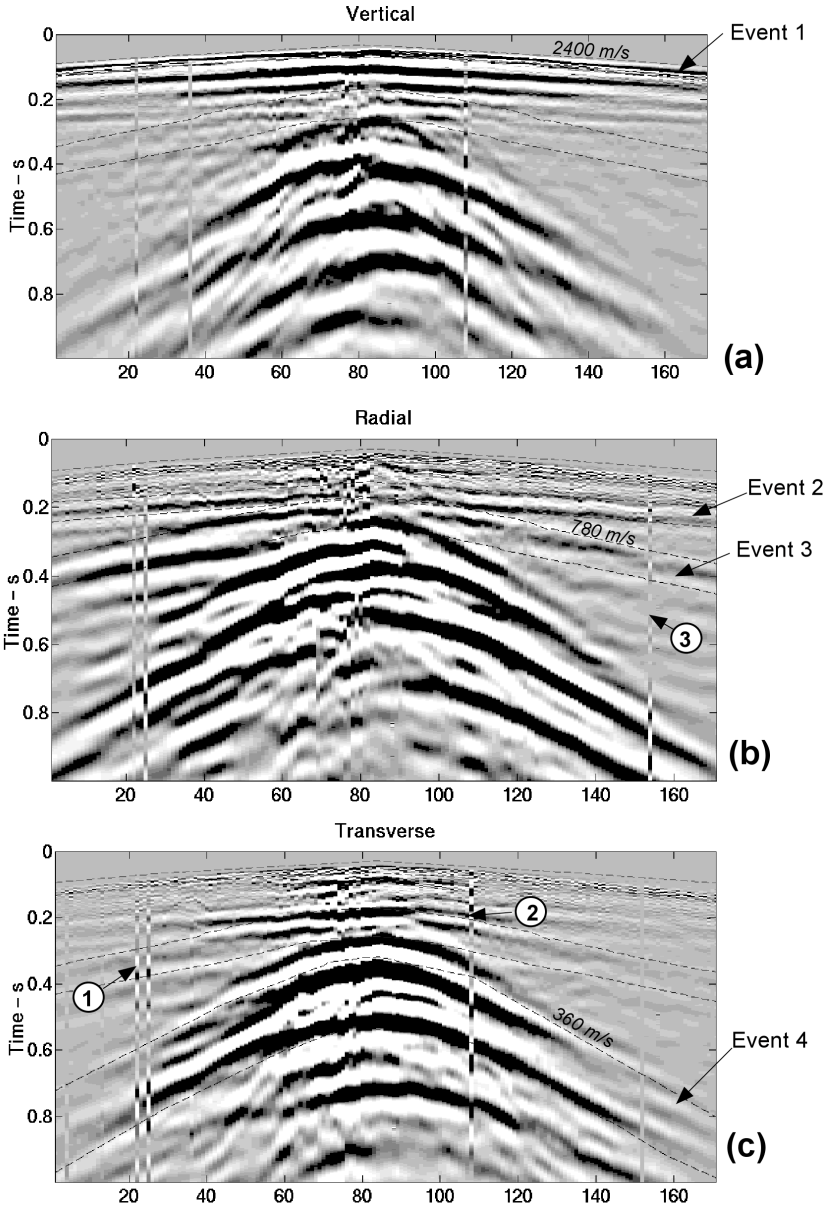

Figure 2. Shot gather in Blackfoot III 3C-3D. (a) Vertical component. (b) Radial (*in-line*) component. (c) Transverse (*Cross-line*) component. Each event and its corresponding analysis window are indicated. The numbers inside circles identify polarity reversals.

The third event (Fig. 5) has a highly linear polarization in the horizontal components (Figures 5*b* and 5*c* and factor ***f1***). The horizontal polarization and the apparent velocity of this event indicate a shear wave refraction, which agrees with the analysis provided by Dufour and Lawton (1996). Receiver 75 shows lower linearity, which can be related to the interference of ground-roll or other wave modes, since this receiver is closer to the source (see location in Figure 2).

Event 4 (Figure 6) also shows good correlation between the source-receiver and polarization angles, and may be ground-roll since it appears more elliptical, with high energy content, and with the appropriate velocity (Fig. 2c).

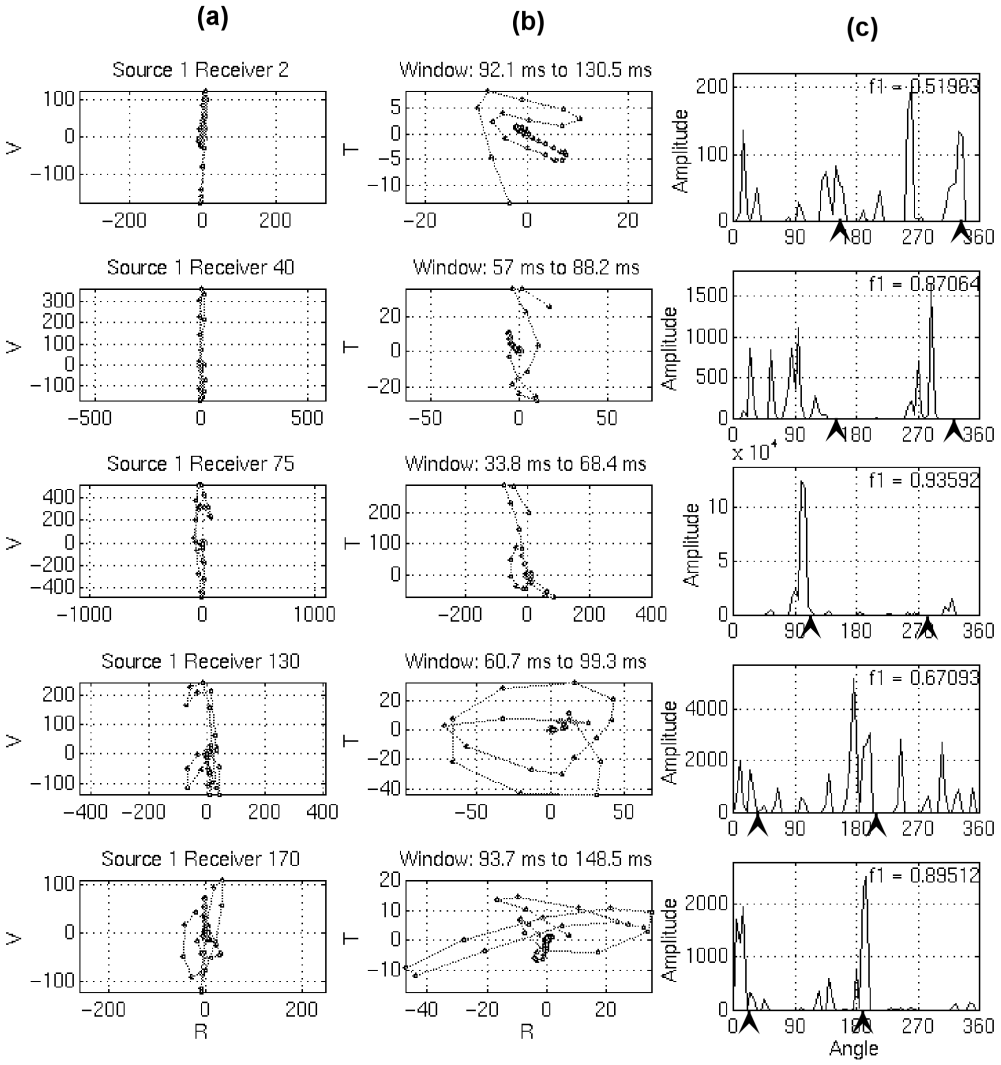

Figure 3. Event 1 analysis: (a) lateral-view hodogram; (b) top-view hodogram; (c) histogram and linearity *f1* from the covariance matrix method. The arrows indicate the source-receiver azimuth obtained from field data.

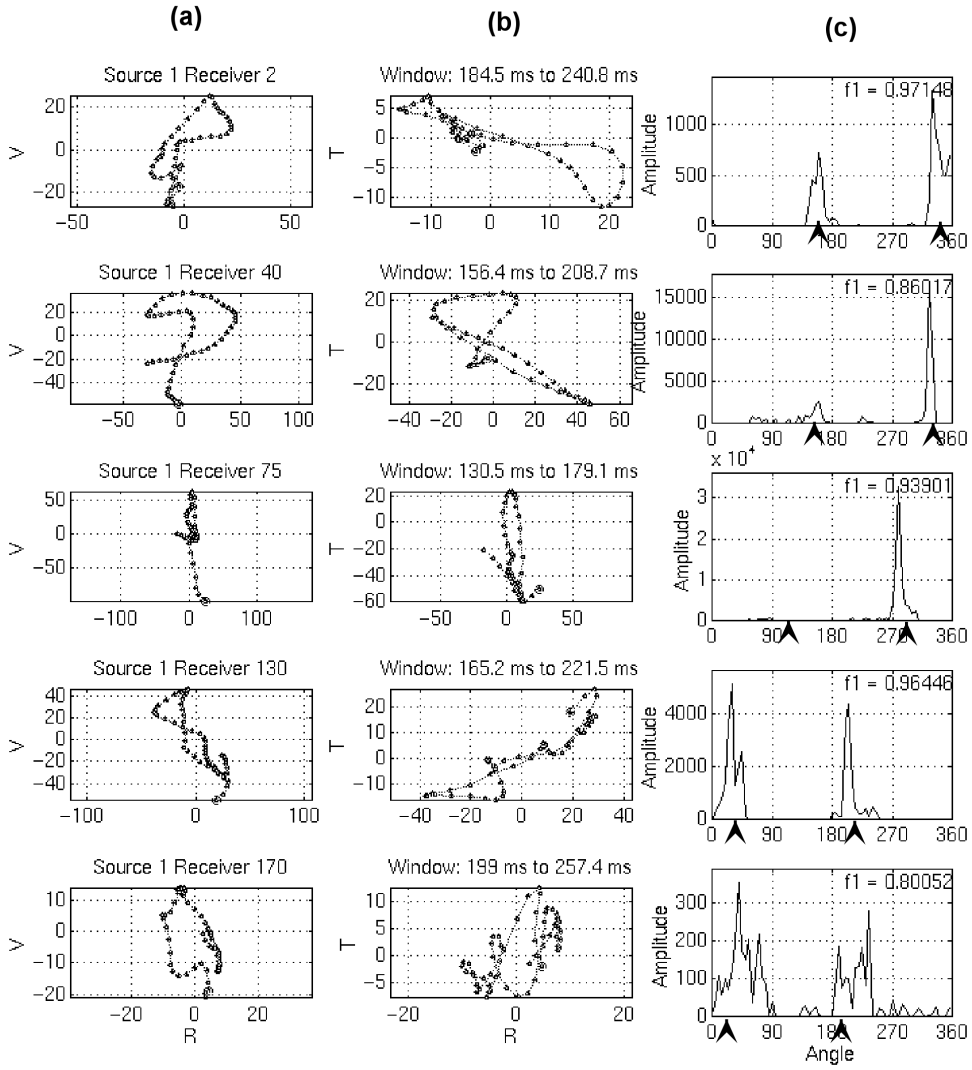

Figure 4. Event 2 analysis: (a) lateral-view hodogram; (b) top-view hodogram; (c) histogram and linearity *f1* (from the covariance matrix method). The arrows indicate the source-receiver azimuth obtained from field data.

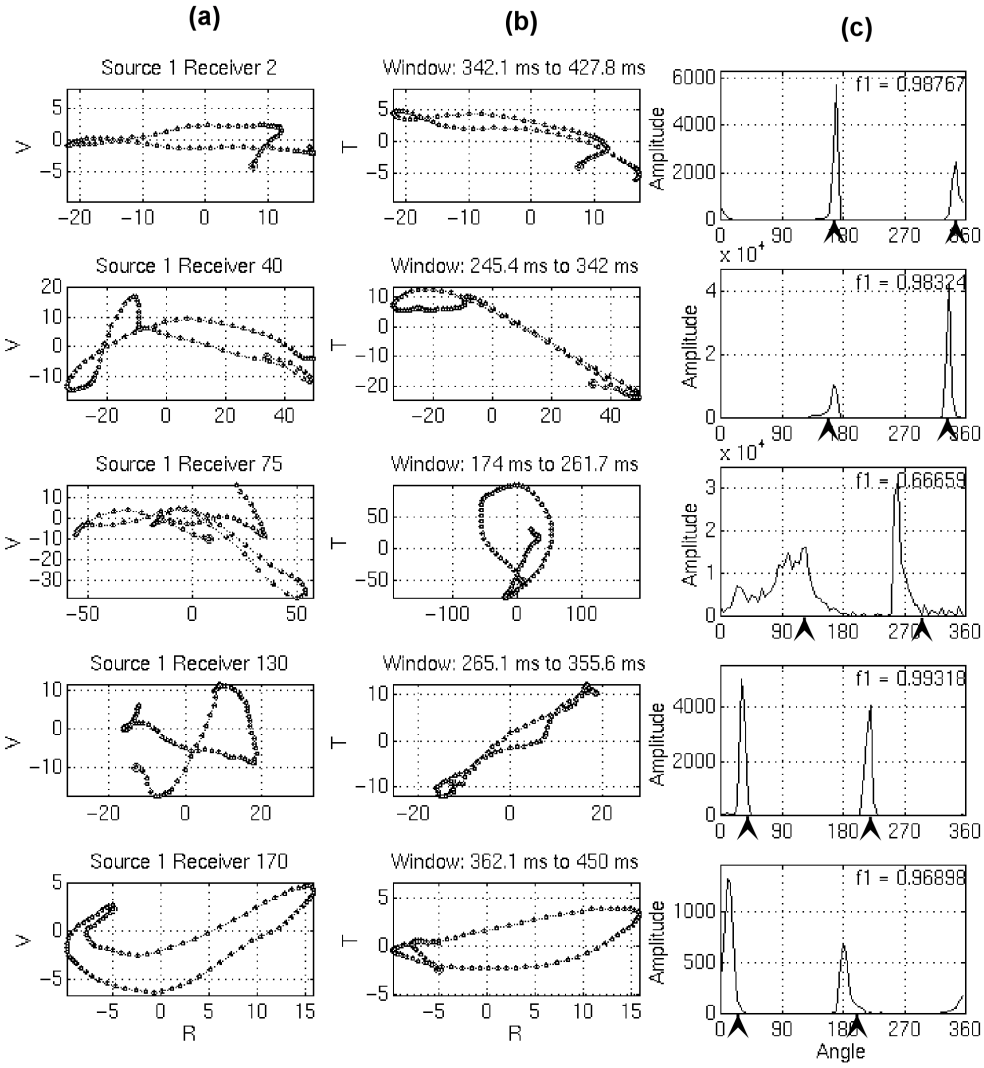

Figure 5. Event 3 analysis: (a) lateral-view hodogram, (b) top-view hodogram, (c) histogram and linearity *f1* from the covariance matrix method. The arrows indicate the source-receiver azimuth from field data.

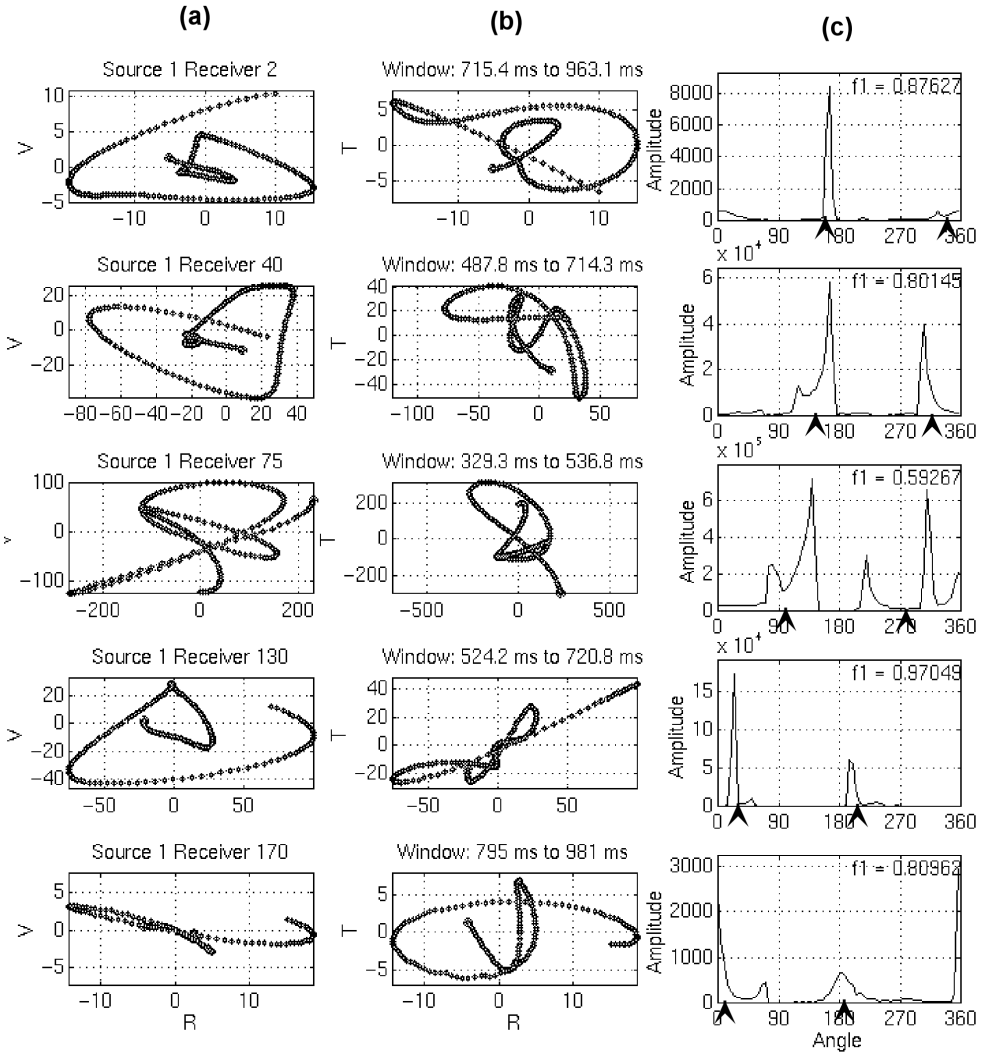

Figure 6. Event 4 analysis: (a) lateral-view hodogram; (b) top-view hodogram; (c) histogram and linearity *f* from the covariance matrix method. The arrows indicate the source-receiver azimuth from field data.

Covariance matrix analysis

Figures 7 to 10 illustrate the results of the second analysis, using the covariance matrix method. To carry out this comparison, the source-receiver azimuths, measured clockwise from the North, were translated to the reference system of the receivers, namely counterclockwise from the radial positive component (R). Table 2 is a comparison of the source-receiver azimuth with polarization on the receivers selected for each one of the four events, calculated with the covariance matrix method.

In all of the events a correlation exists between the calculated source-receiver angle and the horizontal polarization direction. This correlation however is low in the case of event 1, first arrivals (Figure 7), and is high in events 2 to 4 (Figures 8 to 10). Some polarization anomalies, marked with numbers in Figure 9 and identifiable in

Figures 8 and 10, appear related to the trace inversions (i.e. polarity reversals) indicated in Figure 2.

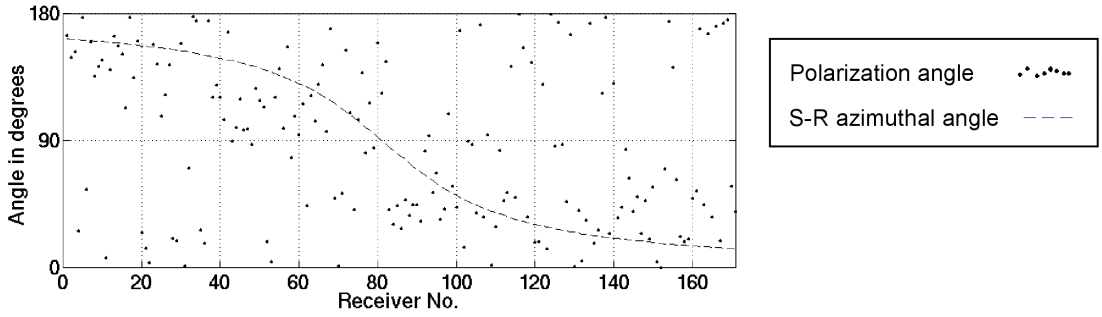

Figure 7. Event 1 polarization and source-receiver angles comparison using the covariance matrix method. The source receiver azimuths were translated to the polarization angles reference system. Low correlation can be observed in this case.

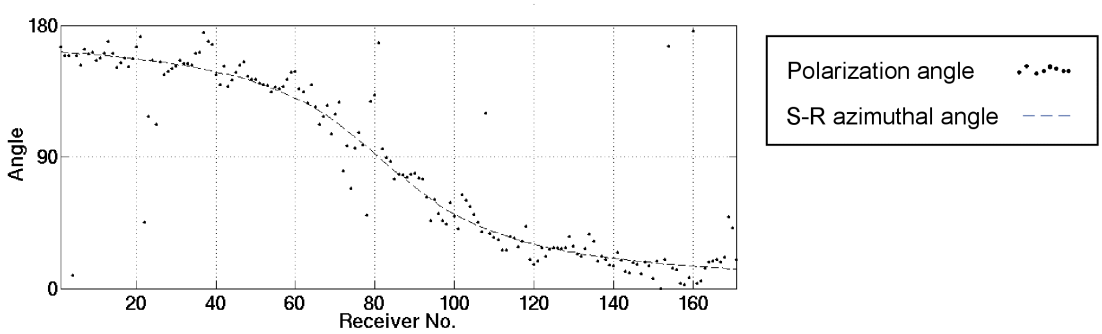

Figure 8. Second event polarization angles and source-receiver angles comparison using the covariance matrix method.

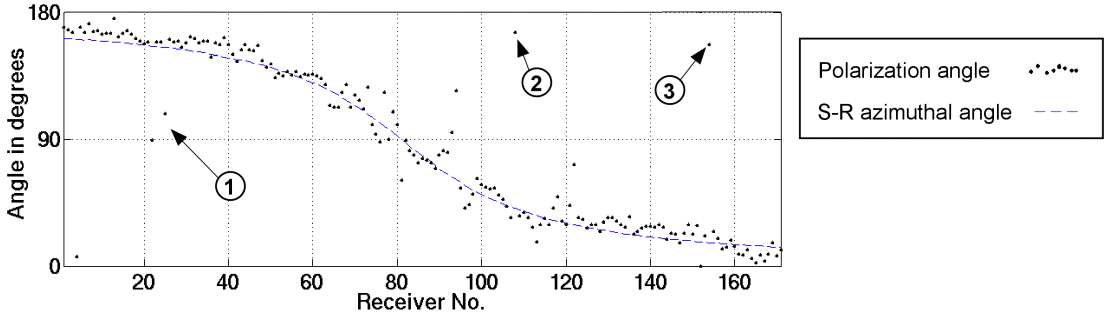

Figure 9. Third event polarization and source-receiver angles comparison using the covariance matrix method. Numbers inside circles indicate polarization anomalies corresponding to polarity reversals in the shot gather (Figure 2).

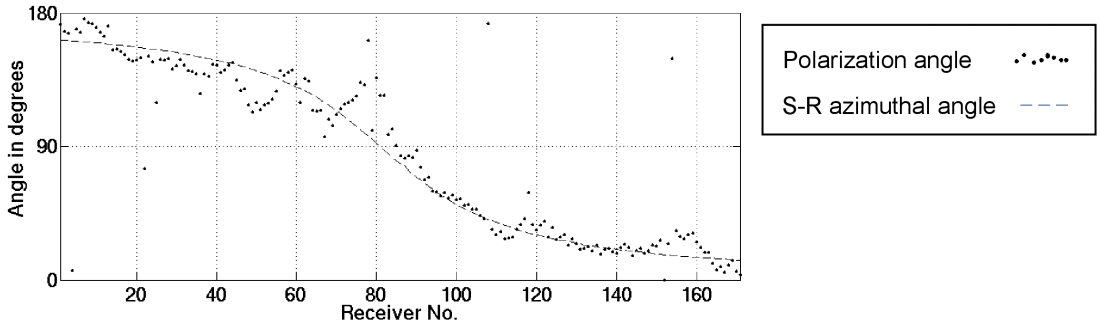

Figure 10. Fourth event (Ground roll) polarization and source-receiver angles comparison using the covariance matrix method.

CONCLUSIONS

The horizontal polarization of three out of four events tested revealed close correlation to the source receiver azimuth. Higher correlation corresponds to horizontally polarized events, such as *S* waves and ground-roll.

This result shows that polarization, as well as for the determination of shot-receiver azimuth, has potential to be used as a part of a robust method for multicomponent geophone orientation.

ACKNOWLEDGEMENTS

We thank the CREWES staff, especially Hanxing Lu and Henry Bland, for technical support and suggestions, and the CREWES sponsors for their financial support. Also the first author thanks ECOPETROL for sponsoring his studies.

REFERENCES

Bland, H.C. and Stewart, R.R., 1996, Geophone orientation, location, and polarity checking for 3-C seismic surveys: CREWES Research Report, **8**, 3-1.

DiSiena, J.P., Gaiser, J.E. and Corrigan, D., 1984, Horizontal components and shear wave analysis of three-component VSP data, *in* Toksoz, N. and Stewart R. R., Editors, Vertical seismic profiling: advanced concepts: Geophysical Press, Vol. **15 B**.

Dufour, J. and Lawton, D., 1996, Refraction analysis of the Blackfoot 2D-3C data: CREWES Research Report, Vol. **8**, 14.1 – 14.32.

Flinn, E.A., 1965, Signal analysis using rectilinearity and direction of particle motion: Proceed. IEEE, **53**, 1874-1876.

Hoffe, B., Stewart, R.R., Bland, H.C., Gallant E.V. and Bertram, M., 1998, The Blackfoot high-resolution seismic survey: design and initial results: SEG 68th Annual Meeting Expanded Abstracts, 103-106.